http://dx.doi.org/10.5012/bkcs.2014.35.2.569

# Effect of Self-Assembled Monolayer Treated ZnO on the Photovoltaic Properties of Inverted Polymer Solar Cells

**Seong Il Yoo, Thu Trang Do, Ye Eun Ha, Mi Young Jo, Juyun Park,† Yong-Cheol Kang,† and Joo Hyun Kim***

*Department of Polymer Engineering and †Department of Chemistry, Pukyong National University, Busan 608-739, Korea*
**E-mail: jkim@pknu.ac.kr*
*Received November 7, 2013, Accepted November 29, 2013*

Inverted bulk hetero-junction polymer solar cells (iPSC) composed of P3HT/$PC_{61}BM$ blends on the ZnO modified with benzoic acid derivatives-based self-assembled monolayers (SAM) are fabricated. Compared with the device using the pristine ZnO, the devices with ZnO surface modified SAMs derived from benzoic acid such as 4-(diphenylamino)benzoic acid (DPA-BA) and 4-(9*H*-carbazol-9-yl)benzoic acid (Cz-BA) as an electron transporting layer show improved the performances. It is mainly attributed to the favorable interface dipole at the interface between ZnO and the active layer, the eective passivation of the ZnO surface traps, decrease of the work function and facilitating transport of electron from PCBM to ITO electrode. The power conversion eciency (PCE) of iPSCs based on DPA-BA and Cz-BA treated ZnO reaches 2.78 and 2.88%, respectively, while the PCE of the device based on untreated ZnO is 2.49%. The open circuit voltage values ($V_{oc}$) of the devices with bare ZnO and SAM treated ZnO are not much different. Whereas, higher the fill factor (*FF*) and lower the series resistance ($R_s$) are obtained in the devices with SAMs modification.

**Key Words :** Self-assembled monolayer, Inverted polymer solar cells, Interface dipole

## Introduction

Polymer solar cells (PSCs) are considered as promising technologies for generating electric power from the sunlight in recent years due to their advantages: the possibility for low cost fabrication based on solution-processible roll-to-roll manufacturing, light weight, mechanical flexibility, tunability of chemical properties.[1-3] In general, PSCs with conventional device architecture consists of a poly(3,4-ethylenedioxythiophene):poly(styrenesulfonate) (PEDOT:PSS) hole-transporting layer and a bulk-heterojunction (BHJ) layer sandwiched between a high work function-hole collecting conducting transparent metal oxide electrode and a low work function-electron collecting metal electrode.[4-6] However, the acidic nature of buffer layer PEDOT:PSS[7,8] and the low work function metal[9-11] in this architecture which result in reduction of device performance. To address these challenges, the previous reports have revealed that the inverted PSC is as a promising alternative for obtaining high device performance, in which high work function metals (such as Ag and Au) are used as the anode while ITO is employed as the bottom cathode.[12-14]

To develop high performance inverted PSCs, the nature of the electrical contacts between the organic semiconducting layer and the electrodes needs to be paid attention because it plays an essential role in determining device characteristics such as the open-circuit voltage ($V_{oc}$), the short-circuit current density ($J_{sc}$), the ll factor (*FF*), the series resistance ($R_s$), and the paralell (shunt) resistance ($R_p$), as well as the power conversion eciency (PCE).[15,16] In order to achieve a good contact (mechanical or electrical contact), various modifications of the electrodes have been investigated, including the introduction of appropriate charge collecting layers between the organic photoactive layer and the electrodes to increase the built-in potential and to decrease the contact resistance. Among the interface materials, semiconducting transition metal oxides are attractive and promising because of their solution processibility as well as their outstanding capability to collect/transfer carriers.[17] Recently, metal oxides such as TiOx and ZnO were introduced between the active layer and cathode as a multifunctional buffer layer for hole blocking[5,17] as well as an optical spacer and oxygen barrier.[18] Compared to TiOx, air stable ZnO has been regarded as one of the promising candidates for the electron selective and hole blocking layer because of its high electron mobility and transmittance.[19] Nevertheless, hydroxyl terminated metal oxides are known to act as traps, which can affect the electrical properties at the interface between the metal oxide and the organic layers.[20,21] Interface modifiers with self-assembled monolayers (SAMs) provide a convenient, flexible method to enhance the charge extraction between the organic layers and the metal oxides through covalently bonding the modiers onto the surface of the metal oxide. By this way, the surface charge traps are passivated which benefit for charge transfer. Besides, it also helps to tune the energy level offset between semiconductors and organic layers, and affect the upper organic layer morphology.[22,23] Previously, a series of benzoic acid derivatives-based SAM modiers with different substituents were formed on the ZnO electron selective layer of polymer BHJ inverted solar cells showing an improved device efficiency was reported.[24,25] It was found that the work function and morphology of the active layer can be controlled by SAM treatment of the ZnO surface with various dipole orientation which contributed by a substituent

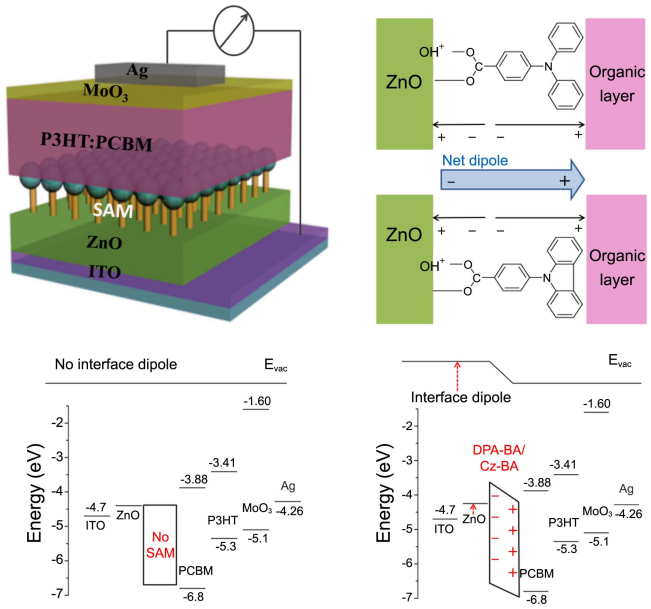


**Figure 1.** Schematic illustration of polymer solar cells with SAM modied ZnO and schematic energy level diagram of the devices with SAM modied ZnO. For ZnO/DPA-BA and ZnO/Cz-BA, the interfacial dipole directed away from ZnO. There is no net interfacial dipole for ZnO without SAM.

on the 4-position of benzoic acid. Compared to the device based on bare ZnO, SAM with an electron withdrawing group (–F) on the benzoic acid modified ZnO forms unfavorable dipole across the ZnO and the active layer results in Schottky contact and shows poorer device performance; Whereas, SAM with electron donating groups (–methoxy, –*tert*-butyl) treated ZnO have a favorable dipole across the ZnO and active layer and generate better contact so that the devices show better performances.

In this research, we synthesized two SAM molecules such as 4-(diphenylamino)benzoic acid (DPA-BA) and 4-(9*H*-carbazol-9-yl)benzoic acid (Cz-BA) which derived from benzoic acid with different rich-electron donating group on the para position to modify ZnO surface. We refer to DPA-BA treated ZnO and Cz-BA treated ZnO as ZnO/DPA-BA and ZnO/Cz-BA, respectively. The schematic representation of SAMs treated ZnO and the device structure of inverted type PSC along with the energy level diagram of the components of the device was shown in Figure 1. This figure depicted that the work function of ZnO can be altered by the SAM treatment. In both of cases, the interface dipole of DPA-BA and Cz-BA treated ZnO are directed away from the ZnO surface which leads to their work functions smaller than that of untreated ZnO. Herein, the effect of SAMs modified ZnO as an electron collection layer on the photovoltaic properties of inverted PSCs will be discussed.

## Experimental Section

**Materials.** All other chemicals were purchased from Sigma-Aldrich Co, Tokyo Chemical Industry (TCI) or Alfa Aesar and used as received unless otherwise described. Regioregular poly(3-hexylthiophene) (P3HT) and (6,6)-phenyl-C61-butyric acid methyl ester ($PC_{61}BM$) were purchased from Rieke Metals Inc. and nano-C Inc., respectively.

**4-(Diphenylamino)benzaldehyde (1).** A portion of 2.16 g (29.5 mmol) of *N*,*N*-dimethyl formamide was added dropwise to a portion of phosphorus oxychloride (4.52 g, 29.5 mmol). The reaction mixture was stirred for 30 minutes at 0 °C. The mixture was added to a solution of triphenylamine (0.48 g, 1.97 mmol) in 10 mL of dichloroethane. Then the reaction mixture was stirred for 12 h at 90 °C. A portion of 100 mL of water was added into the reaction mixture then extracted three times with 50 mL of methylene chloride (MC). The combined organic layer was washed with aqueous sodium carbonate (10 wt %) and then dried over anhydrous magnesium sulfate ($MgSO_4$). The solvent was removed using a rotary evaporator. The yield of white crystal was 0.49 g (92.7%). mp 135.6 °C. $^1$H-NMR (400 MHz, $CDCl_3$) δ 9.80 (s, 1H), 7.69-7.66 (d, *J* = 11.36 Hz, 2H), 7.35-7.31 (t, *J* = 7.68 Hz, 4H), 7.18-7.15 (m, 6H), 7.03-7.01 (d, *J* = 8.8 Hz, 3H), $^{13}$C-NMR (100 MHz, $CDCl_3$) δ 190.29, 153.23, 146.05, 131.21, 129.65, 129.01, 126.21, 125.02, 119.25. Anal. Calcd. For $C_{19}H_{13}NO_2$: C, 79.43; H, 4.56; N, 4.88; O, 11.14. Found: C, 79.82; H, 4.51; N, 4.782.

**4-(Diphenylamino)benzoic acid (DPA-BA).** A portion of compound **1** (0.30 g, 1.097 mmol), hydrogen peroxide (2.5 mL, 1.097 mmol) and sodium hydroxide (0.045 g, 1.097 mmol) was dissolved in 5 mL of dioxane and the mixture was stirred for 2 h at 0 °C. Then the reaction mixture was heated up to 100 °C and stirred for 12 h. The reaction mixture was cooled down the room temperature and filtered. The filtrate was adjusted to pH 2 with HCl solution, and filtered again. The yield of the gray powder was 0.25 g (78.3%). mp 174.9 °C. $^1$H-NMR (400 MHz, MeOH-$d_3$) δ 7.98-7.96 (d, *J* = 8.08 Hz, 2H), 7.33-7.28 (m, 4H), 7.22-7.19 (m, 4H), 7.07-7.02 (t, *J* = 7.32 Hz, 2H), 6.73-6.69 (t, *J* = 8.08 Hz, 2H). Anal. Calcd. For $C_{19}H_{15}NO_2$: C, 78.87; H, 5.23; N, 4.84; O, 11.06. Found: C, 78.51; H, 5.34; N, 4.69.

**4-(9*H*-Carbazol-9-yl)benzaldehyde (2).** A mixture of 4-bromobenzaldehyde (0.231 g, 1.25 mmol), 9*H*-carbazole (0.167 g, 1.00 mmol), copper powder (0.095 g, 1.50 mmol), potassium carbonate (0.207 g, 1.50 mmol) and 18-crown-6 (0.013 g, 0.05 mmol) in 1,2-dichlorobenzene was stirred at 170 °C for 12 hours under the nitrogen atmosphere. After the reaction mixture was cooled down to room temperature, excess of $K_2CO_3$ and Cu is removed by the filtration. A portion of 100 mL of water was added into the filtrate and then extracted three times of with a portion of 100 mL of MC. The combined organic layer was dried over anhydrous $MgSO_4$ then the solvent was removed using a rotary evaporator. The yield of the colorless solid was 0.172 g (63.4%). mp 160.3 °C. $^1$H-NMR (400 MHz, $CDCl_3$) δ 10.10 (s, 1H), 8.16-8.11 (m, 4H), 7.79-7.77 (d, *J* = 8.08 Hz, 2H), 7.52-7.49 (d, *J* = 8.08 Hz, 2H), 7.46-7.42 (t, *J* = 6.96 Hz, 2H), 7.36-7.32 (t, *J* = 7.72 Hz, 2H), $^{13}$C-NMR (100 MHz, $CDCl_3$) δ 190.92, 143.32, 139.99, 134.56, 131.32, 126.74, 126.23, 123.91, 120.77, 120.45, 109.71. Anal. Calcd. For $C_{19}H_{13}NO$: C, 84.11; H, 4.83; N, 5.16; O, 5.90. Found: C, 84.10; H,

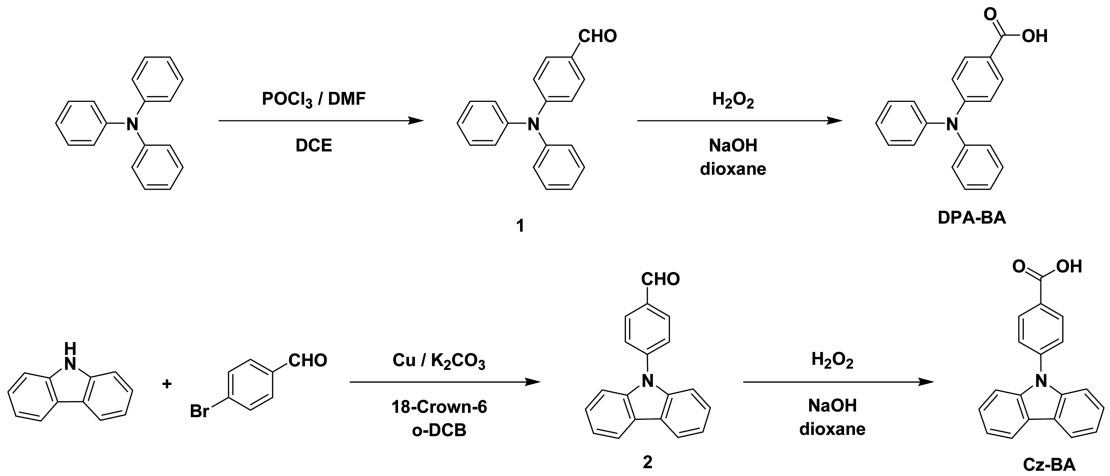


**Scheme 1.** Synthesis route of DPA-BA and Cz-BA.

4.79; N, 5.97.

**4-(9*H*-Carbazol-9-yl)benzoic acid (Cz-BA).** A portion of compound **2** (0.061 g, 0.220 mmol), hydrogen peroxide (0.5 mL, 0.220 mmol) and sodium hydroxide (0.009 g, 0.220 mmol) was dissolved in 1 mL of dioxane and the mixture was stirred for 2 h at 0 °C. Then the reaction mixture was heated up to 100 °C and stirred for 12 h. The reaction mixture was cooled down the room temperature and filtered. The filtrate was adjusted to pH 2 with HCl solution, and filtered again. The crude residue was purified by recrystallization using n-hexane. The yield of the yellowish white solid was 0.034 g (53.7%). mp 213.0 °C. $^1$H-NMR (400 MHz, MeOH-$d_3$) δ 8.31-8.28 (d, $J$ = 8.80 Hz, 2H), 8.15-8.13 (d, $J$ = 7.68 Hz, 2H), 7.72-7.69 (d, $J$ = 8.44 Hz, 2H), 7.47-7.38 (m, 4H), 7.29-7.26 (t, $J$ = 7.68 Hz, 2H). Anal. Calcd. For $C_{19}H_{13}NO_2$: C, 79.43; H, 4.56; N, 4.88; O, 11.14. Found: C, 79.82; H, 4.47; N, 4.79.

**Measurements.** Synthesized compounds were characterized by $^1$H NMR and $^{13}$C NMR spectra, which were obtained with a JEOL JNM ECP-400 spectrometer. The static contact angle of the ZnO layer before and after SAM treatment was measured by deionized water. Elemental analysis of before and after SAM treatment by the benzoic acid derivatives was performed using (THERMO VG SCIENTIFIC (UK), Multi-Lab2000) X-ray photoelectron spectroscopy (XPS) and recorded using Al Kα X-ray line (15 kV, 300 W). The surface roughness and topographic properties of the surfaces of the active layer were characterized with atomic force microscopy (AFM) by using a Digital Instruments (Multi-Mode SPM) operated in the tapping mode. The current density-voltage measurements under 1.0 sun (100 mW/cm$^2$) condition from a 150 W Xe lamp with a 1.5 G lter were performed using a KEITHLEY model 2400 source-measure unit. A calibrated Si reference cell with a KG5 lter certied by the National Institute of Advanced Industrial Science and Technology was used to conrm 1.0 sun condition.

**Fabrication of Device.** PSCs were fabricated in the configuration of the common sandwich structure: ITO/before and after SAM treated ZnO/active layer/$MoO_3$/Ag. The ITO-coated glass substrates were cleaned with deionized water, acetone, methanol, 2-propanol in an ultrasonic bath. After the substrates were dried, they were treated with UV/$O_3$ for 120 s prior to use. A layer of 40 nm thick ZnO film was deposited onto the ITO substrate (sheet resistance = 15 Ω/sq) by using sol-gel process. The sol-gel solution was prepared from a mixture of zinc acetate dehydrate (0.164 g) and ethanolamine (0.05 mL) dissolved in 1 mL of methoxy-ethanol. And then the solution was stirred for 30 min at 60 °C prior to deposition. A layer of 40 nm thick ZnO film was spin-coated on the ITO coated glass and then cured at 300 °C for 10 min to partly crystallize the ZnO lm, which is prepared by the literature procedures.[26,27] Self-assembled molecule was deposited on the ZnO lm by spin-coating a 1.0 mg/mL solution of benzoic acid derivative in methanol at 4000 rpm for 60 s. In order to remove physically absorbed molecules, the SAM treated ZnO surface was washed using pure methanol and then dried by the stream of nitrogen. The photoactive layer was formed from 20 mg of P3HT and 20 mg of $PC_{61}BM$ blend in 1 mL of *o*-dichlorobenzene (ODCB) at 600 rpm for 40 s. The sample was then dried in a covered glass petri dish for 1 h. Prior to spin coating, the active solution was ltered through a 0.45 μm membrane lter. The typical thickness of the active layer was 200 nm. Before the thermal deposition of the $MoO_3$ buffer and the Ag anode, the active layer was thermally annealed at 150 °C for 20 min in the glove box ($N_2$ atmosphere). Finally, 20 nm thick $MoO_3$ and 100 nm thick Ag were deposited successively onto the top of the active layer through a shadow mask with a device area of 0.13 cm$^2$ at 2 × 10$^{-6}$ Torr.

## Results and Discussion

**Characterization of SAM Modied ZnO.** The characteristics of the ZnO and SAMs treated ZnO are analyzed by XPS (X-ray photoelectron spectroscopy). As illustrated Figure 2, the O 1 s peaks can be de-convoluted into three peaks corresponding to the low binding energy (LP), middle binding energy (MP), and high binding energy (HP) components center at 530.11, 531.51, and 532.83 eV, respectively.[28,29] The LP at 530.11 eV is attributed to $O^2$ ions

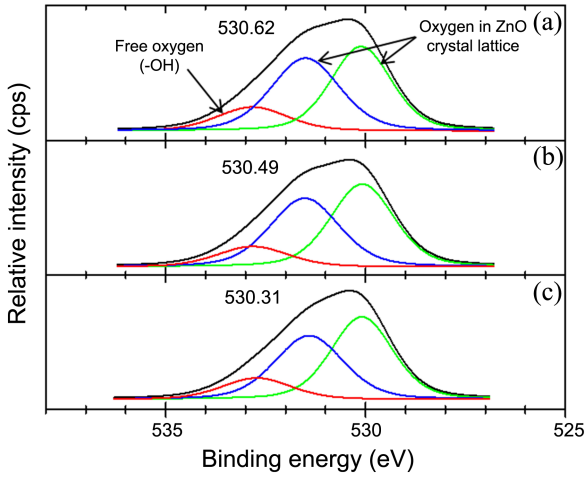


**Figure 2.** XPS spectra of (a) ZnO, (b) DPA-BA treated ZnO, and (c) Cz-BA treated ZnO.

surrounded by Zn in the ZnO crystal lattice system, serving as an indicator of the amount of oxygen atoms in a fully oxidized, stoichiometric environment. The MP, centers at 531.51 eV, is associated with $O^x$ ions ($x < 2$) in the oxygen-deficient regions within the ZnO matrix and is related to oxygen vacancies. The HP, locates at 532.83 eV, is typically attributed to chemisorbed oxygen, dissociated oxygen, or OH groups on the surface. The XPS spectra of ZnO treated with DPA-BA and Cz-BA are depicted in Figure 2(b)-(c) which show that the position of oxygen peaks in SAM modified ZnO are shifted to lower binding energy. It is might be due to the additional presence of O 1s component in the lower binding energy and elimination of zinc hydroxyl bonds (-OH) on the ZnO surface which is a consequence of the chemical absorption between COOH anchor group on SAM molecule and ZnO.[25,30,31] This result indicates that the ZnO surface is covered by Cz-BA and DPA-BA; The defective oxygen vacant sites and the surface hydroxyl groups exposed to the surface of ZnO matrix are replaced by SAMs, mainly through carboxylate bonding.[32] To examine the effects of the SAM treatment on the surface properties of the ZnO layer, we investigate the water contact angle of each sample. The contact angle measurement of hydrophobicity is a well-known indicator of the coverage of a molecular layer on ZnO surface. Without SAM modification, the ZnO surface showed the water contact angle is $45.32 \pm 0.61^o$. Whereas, SAMs treatment onto the ZnO surface is found to become more hydrophobic with a contact angle of $58.82 \pm 1.04^o$ for DPA-BA treated ZnO and $60.40 \pm 0.97^o$ for Cz-BA treated ZnO. The increase in the contact angle possibly due to hydrophobic characteristic of carbazole and diphenylamine substituted benzoate.[33,34] From the contact angle data, we also conrm that SAMs based on benzoic acid derivatives are covered successfully on the ZnO layer.

The charge injection barrier is a very important factor for improving the performances of polymer solar cells. By using electrode interface materials with good charge transporting ability for favorable Ohmic contacts at the interfaces is required to obtain the high $V_{oc}$, $J_{sc}$, and *FF*.[35] In our device

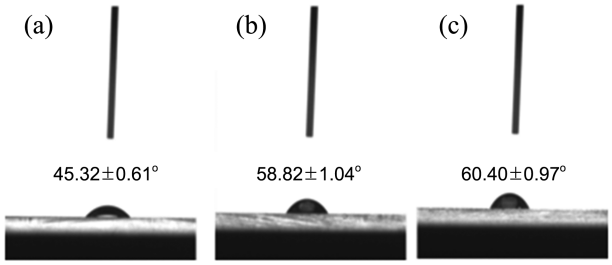


**Figure 3.** Photographs from water contact angle measurements on (a) ZnO, (b) DPA-BA treated ZnO, and (c) Cz-BA treated ZnO.

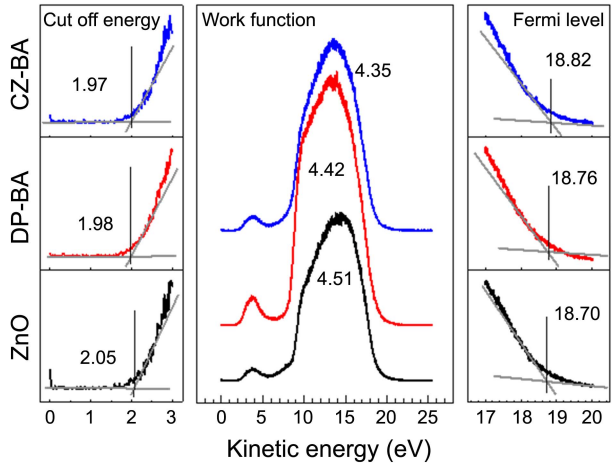


**Figure 4.** UPS spectra of ZnO, DPA-BA treated ZnO, and Cz-BA treated ZnO.

conguration, because the ZnO layer is responsible for the electron collection, a dipolar monolayer with a net dipole directed away from the ZnO is required to reduce the band offset between the conduction band of ZnO and the active layer to achieve Ohmic contact for obtaining a maximized the $V_{oc}$. Devices with a net dipole directed toward the ZnO resulted in an increase of a Schottky barrier, which is expected to decrease the device performance.[36] Herein, we study the effect of SAM treatment on the formation of the interface dipole by measuring the effective work function of ZnO. As shown Figure 4, the effective work function of untreated ZnO, DPA-BA treated ZnO and Cz-BA treated ZnO are 4.51, 4.42 and 4.35 eV, respectively. The direction of interface dipole across the junction depends on the permanent dipole orientation of BA derivatives. In both cases of Cz-BA and DPA-BA, the interface dipole between ZnO and the active layer is directed away from the ZnO. It has been reported that the dipole moment of benzoic acid derivatives was influenced by the 4-substituted groups. When compared to the bare ZnO, the ones modied with benzoic acid containing electron donating groups (–methoxy, –*tert*-butyl) show decrease in the surface potential and the work function of semiconductor while ZnO modied with benzoic acid containing electron withdrawing group (–F) shows an opposite effect.[24] For similar result, the effective work function of ZnO treated with benzoic acid substituted electron donating diphenylamino or carbazole groups are smaller

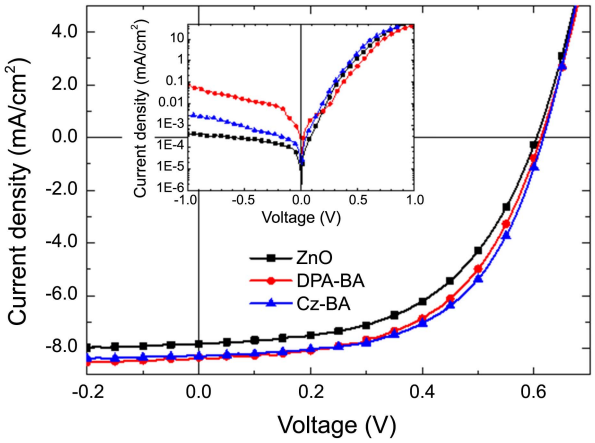


**Figure 5.** Current density-voltage curves of inverted type PSCs under AM 1.5G simulated illumination with intensity of 100 mW/cm$^2$ and under the dark condition (inset) (square, ZnO; circle, DPA-BA treated ZnO; triangle, Cz-BA treated ZnO).

than that of untreated ZnO.

**Photovoltaic Properties.** Figure 5 shows the current density-voltage (J-V) characteristics of the inverted BHJ cells with and without modication of carboxylic acid SAMs under AM 1.5G simulated illumination and under the dark condition. The resulting photovoltaic parameters of the device with the best PCE are summarized in Table 1. From the results, the $V_{oc}$ values of the devices based on ZnO/DPA-BA and ZnO/Cz-BA are 0.61 and 0.62 V, respectively, which are slightly higher than that of device with untreated ZnO (0.60 V). As result, the interfacial dipole formed from the carboxylic acid anchoring to the surface of ZnO does not much affect $V_{oc}$ of devices. The $J_{sc}$ of device with ZnO/DPA-BA and ZnO/Cz-BA show 6.5% and 5.9% enhancement from 7.83 mA/cm$^2$ (untreated ZnO) to 8.34 and 8.29 mA/cm$^2$, respectively. The improved $J_{sc}$ possibly ascribe to benzoic acid-SAM improving the interfacial electron collection by removing the trap states at the interface of the ZnO layer and forming a favorable dipole across the junction between ZnO and the active layer which results in reducing a Schottky barrier.

The enhancement of the PCE of the device with SAMs modifed ZnO is also observed by the improvement of the *FF*. Reducing the hydroxyl groups on the ZnO surface by forming bonds with benzoic acid based SAMs reduces the resistance and recombination losses leading to improvement of the *FF* from 53% to 54.6% and 56.1% for DPA-BA and Cz-BA treated ZnO, respectively. We can recognize that the device with ZnO/Cz-BA manifests the highest *FF*; this is a result of the good contact between layers of device which possesses the lowest $R_s$ and the highest $R_p$ value compared to those of the devices untreated ZnO and ZnO/DPA. The highest values of the $V_{oc}$ and the *FF* induced the best PCE in the device with Cz-BA treated ZnO (2.88%) compared to those of the devices with bare ZnO (2.49%) and DPA-BA treated ZnO (2.78%). The improvements in the performance of the inverted PSCs containing ZnO modified by benzoic acid derivatives can be attributed to the formation of favorable interface dipole at the interface between ZnO and the active layer which facilitates electron collection ability to the ITO. However, the efficiencies of the device with DPA-BA and Cz-BA are still lower than those of device with SAM based benzoic acid modified by methoxy and *tert*-butyl groups which revealed the PCE of 4.34% and 2.94%, respectively, in the same fabricating condition with our previous report.[24]

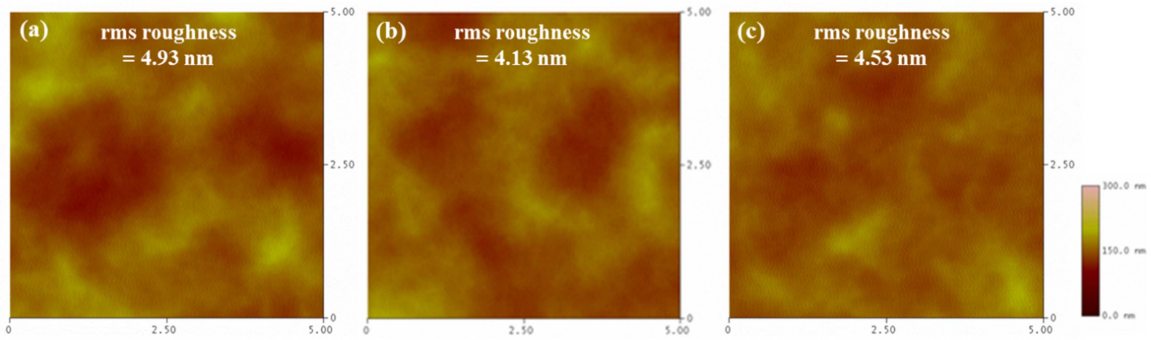


**Figure 6.** AFM topography images of thermally annealed P3HT/PCBM lm on (a) ZnO, (b) ZnO/ DPA-BA, and (c) ZnO/Cz-BA.

**Table 1.** Best photovoltaic parameters and eciencies of PSCs with various SAM treated ZnO

| | $V_{oc}$ (V) | $J_{sc}$ (mA/cm$^2$) | *FF* (%) | PCE (%) | $R_s$ (Ω·cm$^2$)$^a$ | $R_p$ (kΩ·cm$^2$)$^b$ |
|---|---|---|---|---|---|---|
| ZnO | 0.60 | -7.83 | 53.0 | 2.49 | 6.17 | 2.45 |
| | (0.61 ± 0.01) | (-7.80 ± 0.07) | (51.6 ± 1.14) | (2.44 ± 0.07) | | |
| DPA-BA | 0.61 | -8.34 | 54.6 | 2.78 | 4.56 | 23.12 |
| | (0.61 ± 0.004) | (-8.22 ± 0.11) | (53.6 ± 1.17) | (2.71 ± 0.08) | | |
| Cz-BA | 0.62 | -8.29 | 56.1 | 2.88 | 3.07 | 25.67 |
| | (0.62 ± 0.004) | (-8.33 ± 0.06) | (55.8 ± 0.81) | (2.84 ± 0.03) | | |

$^a$Series resistnace (estimated from the devices with best PCE value). $^b$Paralell resistance (estimated from the devices with best PCE value).

This results implies that the simple electron donating groups grafted on benzoic acid are more likely modification for SAM than that of bulky groups.

In order to investigate the effect of SAMs modified ZnO on the surface morphology, we obtained the images by an atomic force microscopy (AFM). As revealed in Figure 5, the r.m.s roughness of P3HT/$PC_{61}$BM blend on the bare ZnO (4.93 nm) is not much different with the r.m.s roughness dats of active layer on DPA-BA (4.13 nm) and ZnO/Cz-BA (4.53 nm). Similarly, the morphology of P3HT/$PC_{61}$BM film processed with benzoic acid based SAMs showed a slight reduction in phase separation is observed in Figure 6(b) and (c). It has been reported that the good miscibility between P3HT and $PC_{61}$BM leads to a large interface for exciton dissociation and bicontinuous interpenetrating networks for free charge transportation, which seems to be consistent with the improved $J_{sc}$ in devices.[37]

## Conclusions

We have demonstrated inverted polymer solar cells based on P3HT:$PC_{61}$BM blends could be fabricated by using solution-processed ZnO treated SAMs as cathode buer layers. As a result, the favorable interface dipole at the interface between ZnO. The facilitation in electron collection from the active layer to the ITO electrode via ZnO led to improve the performances of devices with ZnO treated SAMs. The inverted PSC based on CZ-BA modified ZnO showed the highest results with $V_{oc}$ of 0.62 V, $J_{sc}$ of −8.29 mA/cm$^2$, *FF* of 56.1% and PCE of 2.88%.

**Acknowledgments.** This work was supported by the Pukyong National University Research Fund in 2011 (PK-2011-09). S.I. Yoo and T.T. Do contributed equally to this research.

## References

1. Scharber, M. C.; Mühlbacher, D.; Koppe, M.; Denk, P.; Waldauf, C.; Heeger, A. J.; Brabec, C. J. *Adv. Mater.* **2006**, *18*, 789.
2. Jo, M. Y.; Bae, J. H.; Lim, G. E.; Ha, Y. E.; Katz, H. E.; Kim, J. H. *Synth. Met.* **2013**, *176*, 41.
3. Do, T. T.; Ha, Y. E.; Kim, J. H. *Org. Electron.* **2013**, *14*, 2673.
4. Ma, W.; Yang, C.; Gong, X.; Lee, K.; Heeger, A. J. *Adv. Funct. Mater.* **2005**, *15*, 1617.
5. White, M. S.; Olson, D. C.; Shaheen, S. E.; Kopidakis, N.; Ginley, D. S. *Appl. Phys. Lett.* **2006**, *89*, 143517.
6. Shaheen, S. E.; Brabec, C. J.; Sariciftci, N. S.; Padinger, F.; Fromherz, T.; Hummelen, J. C. *Appl. Phys. Lett.* **2001**, *78*, 841.
7. Wong, K. W.; Yip, H. L.; Luo, Y.; Wong, K. Y.; Lau, W. M.; Low, K. H.; Chow, H. F.; Gao, Z. Q.; Yeung, W. L.; Chang, C. C. *Appl. Phys. Lett.* **2002**, *80*, 2788.
8. Hau, S. K.; Yip, H. L.; Baek, N. S.; Zou, J.; O'Malley, K.; Jen, A. K. Y. *Appl. Phys. Lett.* **2008**, *92*, 253301.
9. Jorgensen, M.; Norrman, K.; Krebs, F. C. *Sol. Energy Mater. Solar Cells* **2008**, *92*, 686.
10. Jorgensen, M.; Norrman, K.; Gevorgyan, S. A.; Tromholt, T.; Andreasen, B.; Krebs, F. C. *Adv. Mater.* **2012**, *24*, 580.
11. Song, M.; Kang, J. W.; Kim, D. H.; Kwon, J. D.; Park, S. G.; Nam, S.; Jo, S.; Ryu, S. Y.; Kim, C. S. *Appl. Phys. Lett.* **2013**, *102*, 143303.
12. Sun, Y.; Seo, J. H.; Takacs, C. J.; Seifter, J.; Heeger, A. J. *Advanced Materials* **2011**, *23*, 1679.
13. Liang, Z.; Zhang, Q.; Wiranwetchayan, O.; Xi, J.; Yang, Z.; Park, K.; Li, C.; Cao, G. *Advanced Functional Materials* **2012**, *22*, 2194.
14. Hu, T.; Li, F.; Yuan, K.; Chen, Y. *ACS Applied Mater & Interfaces* **2013**, *5*, 5763.
15. Blom, P. W. M.; Mihailetchi, V. D.; Koster, L. J. A.; Markov, D. E. *Adv. Mater.* **2007**, *19*, 1551.
16. Chen, S.; Manders, J. R.; Tsang, S.-W.; So, F. *J. Mater. Chem.* **2012**, *22*, 24202.
17. Chen, L. M.; Hong, Z.; Li, G.; Yang, Y. *Adv. Mater.* **2009**, *21*, 1434.
18. Yip, H.-L.; Hau, S. K.; Baek, N. S.; Jen, A. K. Y. *Appl. Phys. Lett.* **2008**, *92*, 193313.
19. Kim, S.; Kim, C. H.; Lee, S. K.; Jeong, J. H.; Lee, J.; Jin, S. H.; Shin, W. S.; Song, C. E.; Choi, J. H.; Jeong, J. R. *Chem. Commun.* **2013**, *49*, 6033.
20. Chua, L. L.; Zaumseil, J.; Chang, J. F.; Ou, E. C. W.; Ho, P. K. H.; Sirringhaus, H.; Friend, R. H. *Nature* **2005**, *434*, 192.
21. Hau, S. K.; Cheng, Y.-J.; Yip, H. L.; Zhang, Y.; Ma, H.; Jen, A. K. Y. *ACS Appl. Mater. Interfaces* **2010**, *2*, 1892.
22. Goh, C.; Scully, S. R.; McGehee, M. D. *J. Appl. Phys.* **2007**, *101*, 114503.
23. Hau, S. K.; Yip, H.-L.; Acton, O.; Baek, N. S.; Ma, H.; Jen, A. K. Y. *J. Mater. Chem.* **2008**, *18*, 5113.
24. Ha, Y. E.; Jo, M. Y.; Park, J.; Kang, Y. C.; Yoo, S. I.; Kim, J. H. *J. Phys. Chem. C* **2013**, *117*, 2646.
25. Song, C. E.; Ryu, K. Y.; Hong, S. J.; Bathula, C.; Lee, S. K.; Shin, W. S.; Lee, J. C.; Choi, S. K.; Kim, J. H.; Moon, S. J. *ChemSusChem* **2013**, *6*, 1445.
26. Bulliard, X.; Ihn, S. G.; Yun, S.; Kim, Y.; Choi, D.; Choi, J. Y.; Kim, M.; Sim, M.; Park, J. H.; Choi, W.; Cho, K. *Adv. Funct. Mater.* **2010**, *20*, 4381.
27. Seo, H. O.; Park, S. Y.; Shim, W. H.; Kim, K. D.; Lee, K. H.; Jo, M. Y.; Kim, J. H.; Lee, E.; Kim, D. W.; Kim, Y. D.; Lim, D. C. *J. Phys. Chem. C* **2011**, *115*, 21517.
28. Xu, C.; Xu, G.; Liu, Y.; Wang, G. *Solid State Commun.* **2002**, *122*, 175.
29. Bang, S.; Lee, S.; Ko, Y.; Park, J.; Shin, S.; Seo, H.; Jeon, H. *Nano. Res. Lett.* **2012**, *7*, 1.
30. Kunat, M.; Girol, S. G.; Burghaus, U.; Woll, C. *J. Phys. Chem. B* **2003**, *2003*, 14350.
31. Perkins, C. L. *J. Phys. Chem. C* **2009**, *113*, 18276.
32. O'Shea, J. N.; Taylor, J. B.; Smith, E. F. *Surf. Sci.* **2004**, *548*, 317.
33. Li, C. Y.; Wen, T. C.; Guo, T. F. *J. Mater. Chem.* **2008**, *18*, 4478.
34. Kaneko, Y.; Fujimori, A. *Chem. Lett.* **2012**, *41*, 1183.
35. Yin, Z.; Zheng, Q.; Chen, S. C.; Cai, D. *ACS Applied Materials and Interfaces* **2013**, *5*, 9015.
36. Yip, H. L.; Hau, S. K.; Baek, N. S.; Ma, H.; Jen, A. K. Y. *Adv. Mater.* **2008**, *20*, 2376.
37. Ma, Z.; Wang, E.; Vandewal, K.; Andersson, M. R.; Zhang, F. *Appl. Phys. Lett.* **2011**, *99*, 143302.